

## Thermal emittance and response time measurements of a GaN photocathode

Ivan V. Bazarov,<sup>1,a)</sup> Bruce M. Dunham,<sup>1</sup> Xianghong Liu,<sup>1</sup> Matt Virgo,<sup>2</sup> Amir M. Dabiran,<sup>3</sup> Fay Hannon,<sup>4</sup> and Hisham Sayed<sup>4</sup>

<sup>1</sup>*Cornell Laboratory for Accelerator-Based Sciences, Cornell University, Ithaca, New York 14853, USA*

<sup>2</sup>*Argonne National Laboratory, Argonne, Illinois 60439, USA*

<sup>3</sup>*SVT Associates, Eden Prairie, Minnesota 55344, USA*

<sup>4</sup>*Thomas Jefferson National Accelerator Facility, Newport News, Virginia 23606, USA*

(Received 30 January 2009; accepted 26 February 2009; published online 23 April 2009)

We present the measurements of thermal emittance and response time for a GaN photocathode illuminated with 5 ps pulses at 260 nm wavelength. The thermal emittance was measured downstream of a 100 kV dc gun using a solenoid scan with a wire scanner and a beam viewscreen and was found to be  $1.35 \pm 0.11$  mm mrad normalized rms emittance per 1 mm rms of illuminated spot size. The response time of the photoemitted electrons was evaluated using a deflecting mode rf cavity synchronized to the laser pulses and was found to be prompt within the time resolution capability of our setup. © 2009 American Institute of Physics. [DOI: [10.1063/1.3110075](https://doi.org/10.1063/1.3110075)]

### I. INTRODUCTION

Gallium nitride (GaN) is a wide band gap (3.4 eV) semiconductor generally deposited as a thin film onto a sapphire substrate by metalorganic chemical vapor deposition or molecular beam epitaxy. The processes necessary to fabricate high quality GaN were developed during the 1990s as part of an intense effort to demonstrate practical blue light-emitting diodes (LED) and laser diodes. Since that time, the photoemissive properties of GaN have been investigated.<sup>1-3</sup> Like GaAs, it is a negative electron affinity (NEA) emitter;<sup>4,5</sup> high quantum efficiency (QE) is achieved by coating the surface with cesium, which lowers the conduction band minimum (CBM) at the surface below the vacuum level. As a photoemitter, GaN has a number of interesting characteristics. Its QE was found to be above 40% with near-UV illumination.<sup>1,6</sup> It was found to be resistant to vacuum contamination.<sup>7</sup> It is also readily activated to NEA, requiring only cesium, which forms a stable layer, in contrast to requiring activation by successive applications of cesium and NF<sub>3</sub> or N<sub>2</sub>O in the case of GaAs.<sup>8</sup> The main drawback is that they require UV illumination. The band gap of 3.4 eV corresponds to a wavelength of 354 nm and a slightly shorter wavelength is required for high quantum efficiency. Because solid state and fiber drive lasers rely on nonlinear crystals to generate visible and UV wavelengths and because these crystals absorb UV light, the average laser power that can be generated at these wavelengths is limited. However, the band gap of GaN can be reduced by the incorporation of indium (InGaN), so further advances in III-nitride fabrication will push the threshold wavelength for these emitters toward the visible spectrum.

Two other important aspects of photocathodes when used in applications requiring high brightness electron bunches of a short duration are small transverse emittance and prompt response of photoemitted electrons.<sup>9</sup> These two

characteristics eventually set the limit to achievable electron beam brightness from photoinjectors,<sup>10</sup> a key parameter for several novel accelerator-based applications such as linac-based synchrotron radiation sources and electron-ion colliders. In this work we present the experimental results evaluating the GaN photocathode performance as a cathode for a high-brightness photogun in terms of its intrinsic (thermal) emittance and time response when illuminated with 260 nm photons.

In this paper, Sec. II contains a description of the GaN samples and the experimental setup used in this work. The results of these measurements are presented in Sec. III followed by a discussion.

### II. EXPERIMENTAL SETUP

The setup used in this work and the related experimental methods have been detailed elsewhere.<sup>9,11</sup> The experimental setup consists of a high voltage dc photoemission gun followed by a diagnostic beamline capable of transverse and longitudinal profile characterization of the electron beam. Beam emittance was measured at 100 kV dc gun voltage using a solenoid scan of two identical solenoid magnets with opposite axial field direction to cancel the overall Larmor's angle. The beam profile at each solenoid setting was measured using a chemical vapor deposition (CVD) diamond viewscreen with 12 bit camera and also a wire scanner. The viewscreen and wire scanner were situated 3.08 and 2.78 m from the cathode, respectively. A 260 nm laser illuminated a circular aperture, which was imaged without magnification onto the cathode. Four different diameter apertures ranging from 1 to 2.6 mm were used. A low current electron beam of less than 1  $\mu$ A was extracted from GaN cathode and aligned to pass through the center of each solenoid to avoid the effect of asymmetrical fields. The measured transverse profiles for both the beam and the laser spot have been computed after the appropriate background subtraction procedure.<sup>9</sup>

GaN (*p*-type) photocathode structures were grown on

<sup>a)</sup>Electronic mail: [ib38@cornell.edu](mailto:ib38@cornell.edu).

*c*-plane sapphire at SVT Associates (SVTA) in a molecular beam epitaxy (MBE) system equipped with effusion ovens for evaporating elemental materials including Ga and Al for thin film growth and Mg for *p*-type doping. Active nitrogen for growth was provided by a rf plasma source (SVTA-RF45). During growth, reflection high-energy electron diffraction was used to monitor surface morphology. Other *in situ* measurements including emissivity-corrected surface temperature, thin film growth rate, and III/V flux ratio were performed by a combination of emissivity-corrected pyrometry and two-color reflectometry (SVTA-IS4000). The growth process started with surface nitridation of the sapphire substrate at 800 °C using the rf plasma source followed by the growth of a thin AlN nucleation layer. Next, up to 1  $\mu\text{m}$  of high-quality GaN buffer was grown. Finally, 0.5  $\mu\text{m}$  of Mg-doped GaN was grown at 650 °C. The Mg doping was adjusted for very high *p*-type doping without forming Mg precipitate related defects. Under optimized growth conditions used, van der Pauw–Hall measurements indicated *p*-type conductivity with carrier density near  $1 \times 10^{19} \text{ cm}^{-3}$ .

Some of the *p*-GaN wafers were processed at SVTA to fabricate 35 mm diameter photocathodes with a 5 mm contact metal ring at the perimeter. To minimize surface contamination and eliminate the need for aggressive cleaning for the NEA photocathode activation process by Cs deposition, a chemical-free process was used to form the Ohmic contact ring by depositing 30 nm of Ni and then 100 nm of Au by electron beam evaporation through a shadow mask. The Ohmic contact was then improved by rapid thermal annealing at 500 °C in a nitrogen atmosphere for 30 s. Finally the wafers were cut by diamond saw into photocathodes with suitable shape for installing in the electron gun. The GaN wafer was etched in sulfuric acid at 70 °C for 5 min before being indium soldered onto the puck. After a 200 °C vacuum bakeout in the load-lock chamber, the cathode was then transferred into the heat cleaning chamber and heated at 600 °C for 90 min. After cooling to room temperature, it was activated using cesium until the maximum photocurrent was obtained using a 300 nm UV LED as a light source. The QE obtained at 300 nm was 14%. The “semi-yo-yo” procedure using alternating layers of Cs and NF<sub>3</sub>, which we normally used for the GaAs photocathode, was tried on our test GaN cathodes but showed no significant effects on the QE.

For the emittance and time response measurements, a Yb-fiber laser was used with a wavelength of 1060 nm operating at 50 MHz repetition rate<sup>12</sup> and followed by two stages of second-harmonic generation resulting in 260 nm pulses. Autocorrelation pulse measurements at 520 nm indicate a pulse of 2.3 ps full width at half maximum. An additional pulse lengthening occurs in the process of frequency doubling to UV due to group velocity dispersion mismatch, which is estimated to be 4.9 ps for 8 mm optical crystal length. The laser illuminated a circular aperture, which was imaged at 1:1 onto the photocathode. Emittance was measured using the solenoid scan. Refer to Ref. 9 for details on the experimental method. Transverse profile measurements were obtained using both the wire scanner and the viewscreen to allow for a consistency check. Maximum beam cur-

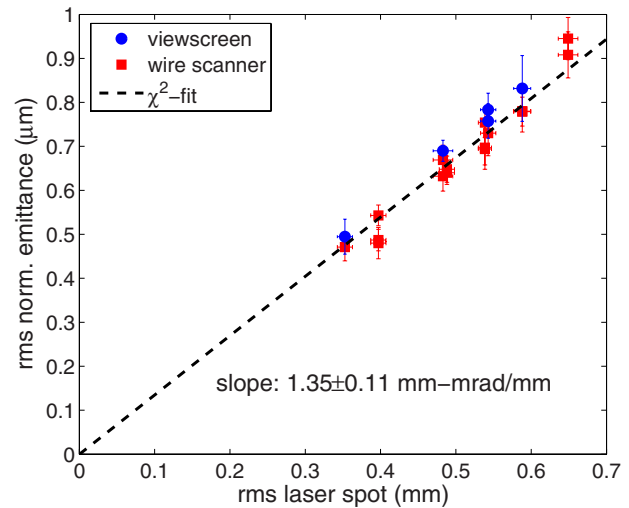


FIG. 1. (Color online) Measured thermal emittance from GaN photocathode excited with 260 nm light for different laser spot sizes. Dashed line shows  $\chi^2$ -fit to determine the slope.

rent used with the wire scanner was 0.9  $\mu\text{A}$  for the largest aperture. Since our analysis assumes negligible space charge in beam propagation, care was taken to evaluate the possible contribution of the space charge for calculated transfer matrices used in emittance retrieval algorithm.<sup>9</sup> The largest error due to the space charge contribution was determined to be no greater than 4% by comparing the results of emittance determined through solenoid scans on simulated data using particle tracking with and without space charge forces taken into account.

Time response measurements of the electron pulse emitted from the cathode were performed using a transverse deflecting rf cavity synchronized to the laser pulse train,<sup>13</sup> which translates the time domain information to the spatial domain. These measurements were done at low enough currents (several nanoamperes) using a highly sensitive BeO viewscreen so that the space charge effects did not affect the temporal profile of bunches leaving the photocathode.

### III. RESULTS

Figure 1 shows the results of thermal emittance measurements for various aperture sizes. The  $\chi^2$ -fit to the data yields  $1.35 \pm 0.11 \text{ mm mrad}$  normalized thermal emittance per 1 mm rms laser spot size (contribution of systematic measurement uncertainty included).

Figure 2 shows the measured temporal profile of the bunch. The measured temporal profile duration  $\sigma_t = 2.2 \text{ ps}$  is fully accounted for by the laser pulse width, indicating that the electron pulse closely follows the laser timing. The resolution of the timing measurement in this case has two components to it, namely, the size of the electron beam spot without the deflecting cavity on and the laser to rf synchronization. The equivalent temporal spread to the timing measurement due to these contributions is estimated to be about 0.8 ps rms. The calibration of the timing scale has been performed by introducing a known delay in the laser path, which allowed us to determine it with an accuracy of better than 5%. Note the absence of a temporal tail, a common

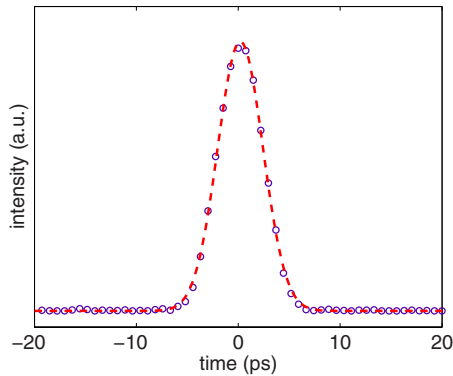


FIG. 2. (Color online) Measured (circles) temporal profile from GaN illuminated by 260 nm wavelength laser light. Dashed line shows Gaussian fit with  $\sigma_t=2.2$  ps. The measured width is due to the laser pulse duration.

feature to NEA photocathodes, due to electron diffusion prior to emission such as that seen in GaAs when illuminated by photons with a near band gap energy.<sup>14</sup>

#### IV. DISCUSSION

Previously, we have reported the measurement data<sup>9</sup> for GaAs obtained for photon energies exceeding its band gap by 0.018–1.3 eV. Transverse thermal energy  $k_B T_{\perp}$ , defined as  $k_B T_{\perp} \equiv m_e c^2 (\epsilon_{n,\perp} / \sigma_{\perp})^2$  (here  $\epsilon_{n,\perp}$ ,  $\sigma_{\perp}$ , and  $m_e c^2$  are rms normalized emittance, rms laser spot size on the photocathode, and electron's rest mass energy, respectively), was found to vary from 0.030 to 0.15 eV over those photon energies. Measurements done for GaAs<sub>0.55</sub>P<sub>0.45</sub> with photons in a range up to 0.7 eV above the direct band gap resulted in  $k_B T_{\perp}$  of 0.13–0.23 eV, which weakly depended on the photon energy but was very sensitive to the surface condition (NEA). For GaN in this work, we have obtained a single data point with photons of 1.4 eV above the band gap with a surprisingly high  $k_B T_{\perp} = 0.9$  eV. All else being equal, the increase in photon energy does not seem sufficient to account for the entire increase in the effective thermal energy of the distribution implied by the higher emittance value for the beam generated from the GaN cathode. Here we discuss which material properties may cause the two families of cathodes to behave differently in this situation.

Electrons excited by photons with energy greater than the band gap lose energy through inelastic collisions until they are emitted or until they reach the CBM, and, eventually, the valence band. The path of each electron is a random walk; the total length of the path traveled by an electron before it reaches a given point greatly exceeds the straight line distance between the points. The number of collisions an electron experiences before it is emitted is thus a function of its initial distance from the surface (absorption depth) and the mean free path between collisions. The total energy dissipated prior to emission is the product of the number of collisions and the energy loss per collision.

For previous emittance measurements made with a GaAs cathode, the highest photon energy used was 2.7 eV. The absorption coefficient for 2.7 eV photons<sup>15</sup> is about  $2 \times 10^5$  cm<sup>-1</sup>. The optical properties of GaN have not been characterized as extensively as those of GaAs; however, ex-

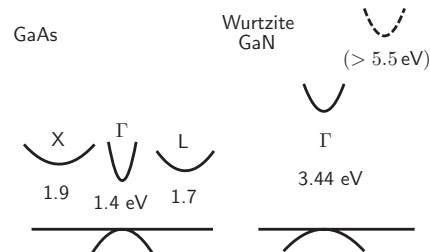


FIG. 3. Band structure in GaAs (left) and GaN (right).

perimentally obtained absorption data are available. For the photon energy used here (4.8 eV), the absorption coefficient<sup>16</sup> is, coincidentally, also roughly  $2 \times 10^5$  cm<sup>-1</sup>, so the photoelectrons are being generated at about the same distance from the surface in both materials. Given that the absorption coefficients are similar in these wavelength ranges, we next consider the scattering mechanisms. For GaAs, several conduction band valleys are accessible for the photon energies under consideration and the scattering rate depends on which region of the Brillouin zone the electron occupies. The CBM is at  $\Gamma$  and above that lie the  $L$  valley (290 meV above the CBM) and the  $X$  valley (480 meV above the CBM) followed by the  $X$  minimum in the second conduction band (890 meV above the CBM).<sup>17</sup> See Fig. 3. The band gap is 1.42 eV so the threshold for photoemission is 877 nm and the upper valleys become accessible with 726, 653, and 539 nm illuminations, respectively. In the  $\Gamma$  valley, the electron mass<sup>18</sup> is  $0.063m_e$  while the density of state effective mass for the  $L$  valley is  $0.56m_e$  and for the  $X$  valley is  $0.85m_e$ .

For the photon energies of interest, direct transitions are only allowed to the central valley. Electrons with enough energy scatter rapidly into the higher valleys where the density of states is greater. Once there, intervalley scattering dominates and the scattering rate<sup>19</sup> is very high ( $1/\tau = 10^{14}$  s<sup>-1</sup>) with each collision resulting in an energy loss<sup>20</sup> of 29 meV. The distribution of electrons among the valleys is strongly influenced by the relative density of states. Because the density of states falls near the bottom of a valley, electrons eventually are more likely to scatter out than in. This may not be true, however, for transitions from the second lowest lying ( $L$ ) valley to the lower density  $\Gamma$  valley: an accumulation of electrons in the  $L$  valley is sometimes<sup>21</sup> (although not always<sup>19</sup>) seen in energy distribution curve data for GaAs.

By contrast, the second lowest conduction band valley of GaN is roughly 2 eV above the CBM,<sup>22</sup> so intervalley scattering does not occur. Emission of 92 meV polar optical phonons<sup>23</sup> is the dominant energy loss mechanism for hot electrons. Applying the model<sup>20</sup> developed by Fröhlich, Callen, and Ehrenreich using the properties of GaN collected in the review by Strite and Morkoç,<sup>24</sup> we find that the scattering rate for electrons with energies exceeding the band gap by 1–1.5 eV, as would be the case here, is on the order of  $10^{14}$  s<sup>-1</sup>, roughly the same as the rate for intervalley scattering in GaAs.

Although scattering rates are similar for both materials at these wavelengths, the average electron velocity under these

conditions is significantly higher in GaN, so the mean free path is longer. The electron effective mass<sup>22</sup> in GaN is  $0.2m_e$ , considerably lower than it is in the satellite valleys of GaAs. Also, because of the presence of higher valleys, the GaAs electrons spend more of their time close to the bottom of a valley. We conclude that because the absorption coefficient is about the same in both cases but the mean free path is longer in GaN, the electrons will reach the GaN surface on average after substantially fewer collisions. The behavior of GaN must be studied at lower photon energies to determine how it would perform as a photoinjector cathode. We mention here two effects which may be observed. Because the rate of polar optical phonon emission drops when the electron energy nears the phonon energy and because the phonon energy is greater than the room temperature thermal energy of the lattice, the electron distribution is unlikely to have enough time to thermalize completely when the emission is prompt. A more speculative but possibly more significant factor may turn out to be scattering in the band bending region. These events can potentially randomize the correlated momentum gained in the direction of the surface due to acceleration through the dipole layer.<sup>25,26</sup> Because the vacuum level falls farther below the bulk CBM in GaN than GaAs [1.2 V versus 0.2–0.5 eV (Refs. 19 and 27)], an effect of this nature would be more pronounced in GaN. If it were of a sufficient magnitude, the emittance would be elevated even under near band gap illumination.

A prompt temporal response from a NEA photocathode may be indicative of a less than complete thermalization of photoemitted electrons, as seen in the case of GaAs illuminated by light of different photon energies below the band gap.<sup>9,11,14</sup> However, within the temporal resolution of our setup, both GaN illuminated with 260 nm and GaAs illuminated with 520 nm light display a prompt response (even though GaAs was found to have a weak temporal tail from 520 nm wavelength illumination for cases of high ( $\geq 10\%$ ) quantum efficiencies<sup>11</sup>).

In summary, we have presented the results of experimental investigation of GaN intrinsic emittance and photoemission response time. This information is relevant to projects seeking to utilize high QE photocathodes in photoinjectors delivering high brightness relativistic electron bunches. Possible physical mechanisms that would lead to an elevated transverse energy of photoelectrons compared to GaAs have been discussed. A more quantitative model is being developed to explain the observed emittance values.

## ACKNOWLEDGMENTS

We acknowledge Dimitre Ouzounov for the laser system support, Yulin Li and Karl Smolenski for their technical

support. This work is supported by NSF (Grant No. PHY-0131508) and NSF/NIH-NIGMS (Award No. DMR-0225180). The work at SVTA is partially supported by DOE (Grant No. DE-FG02-06ER84506).

<sup>1</sup>F. Machuca, Y. Sun, Z. Liu, K. Ioakeimidi, P. Pianetta, and R. F. W. Pease, *J. Vac. Sci. Technol. B* **18**, 3042 (2000).

<sup>2</sup>O. H. W. Siegmund, A. S. Tremsin, A. Martin, J. Malloy, M. P. Ulmer, and B. Wessels, *Proc. SPIE* **5164**, 134 (2003).

<sup>3</sup>F. S. Shahedipour, M. P. Ulmer, B. W. Wessels, C. L. Joseph, and T. Nihashi, *IEEE J. Quantum Electron.* **38**, 333 (2002).

<sup>4</sup>M. Eyckeler, W. Mönch, T. U. Kampen, R. Dimitrov, O. Ambacher, and M. Stutzmann, *J. Vac. Sci. Technol. B* **16**, 2224 (1998).

<sup>5</sup>C. I. Wu and A. Kahn, *J. Appl. Phys.* **86**, 3209 (1999).

<sup>6</sup>S. Uchiyama, Y. Takagi, M. Niigaki, H. Kan, and H. Kondoh, *Appl. Phys. Lett.* **86**, 103511 (2005).

<sup>7</sup>F. Machuca, Z. Liu, J. R. Maldonado, S. T. Coyle, P. Pianetta, and R. F. W. Pease, *J. Vac. Sci. Technol. B* **22**, 3565 (2004).

<sup>8</sup>C. K. Sinclair, P. A. Adderley, B. M. Dunham, J. C. Hansknecht, P. Hartmann, M. Poelker, J. S. Price, P. M. Rutt, W. J. Schneider, and M. Steigerwald, *Phys. Rev. ST Accel. Beams* **10**, 023501 (2007).

<sup>9</sup>I. Bazarov, B. Dunham, Y. Li, X. Liu, D. Ouzounov, C. Sinclair, F. Hannon, and T. Miyajima, *J. Appl. Phys.* **103**, 054901 (2008).

<sup>10</sup>I. Bazarov, B. Dunham, and C. Sinclair, *Phys. Rev. Lett.* **102**, 104801 (2009).

<sup>11</sup>I. V. Bazarov, D. G. Ouzounov, B. M. Dunham, S. A. Belomestnykh, Y. Li, X. Liu, R. E. Meller, J. Sikora, C. K. Sinclair, F. W. Wise, and T. Miyajima, *Phys. Rev. ST Accel. Beams* **11**, 040702 (2008).

<sup>12</sup>D. G. Ouzounov, I. V. Bazarov, B. M. Dunham, C. K. Sinclair, S. Zhou, and F. Wise, Proceedings of the Particle Accelerator Conference, Albuquerque, NM, 2007 (unpublished), p. 530.

<sup>13</sup>S. A. Belomestnykh, V. D. Shemelin, K. W. Smolenski, and V. Veshcherevich, Proceedings of the Particle Accelerator Conference, Albuquerque, NM, 2007 (unpublished), p. 2331.

<sup>14</sup>P. Hartmann, J. Bermuth, D. v. Harrach, J. Hoffmann, S. Kbis, E. Reichert, K. Aulenbacher, J. Schuler, and M. Steigerwald, *J. Appl. Phys.* **86**, 2245 (1999).

<sup>15</sup>D. Aspnes and A. Studna, *Phys. Rev. B* **27**, 985 (1983).

<sup>16</sup>J. F. Muth, J. H. Lee, I. K. Shmagin, R. M. Kolbas, H. C. Casey, Jr., B. P. Keller, U. K. Mishra, and S. P. Denbaars, *Appl. Phys. Lett.* **71**, 2572 (1997).

<sup>17</sup>D. Aspnes, *Phys. Rev. B* **14**, 5331 (1976).

<sup>18</sup>I. Vurgaftman, J. Meyer, and L. Ram-Mohan, *J. Appl. Phys.* **89**, 5815 (2001).

<sup>19</sup>H.-J. Drouhin, C. Hermann, and G. Lampel, *Phys. Rev. B* **31**, 3859 (1985).

<sup>20</sup>E. M. Conwell, *High Field Transport in Semiconductors* (Academic, New York, 1976).

<sup>21</sup>L. James and J. Moll, *Phys. Rev.* **183**, 740 (1969).

<sup>22</sup>M. Goano, E. Bellotti, E. Ghillino, G. Ghione, and K. Brennan, *J. Appl. Phys.* **88**, 6467 (2000).

<sup>23</sup>R. Joshi, S. Viswanadha, P. Shah, and R. del Rosario, *J. Appl. Phys.* **93**, 4836 (2003).

<sup>24</sup>S. Strite and H. Morkoç, *J. Vac. Sci. Technol. B* **10**, 1237 (1992).

<sup>25</sup>Z. Liu, F. Machuca, P. Pianetta, W. E. Spicer, and R. F. W. Pease, *Appl. Phys. Lett.* **85**, 1541 (2004).

<sup>26</sup>D. A. Orlov, M. Hoppe, U. Weigel, D. Schwalm, A. S. Terekhov, and A. Wolf, *Appl. Phys. Lett.* **78**, 2721 (2001).

<sup>27</sup>F. J. Machuca, "A thin film *p*-type GaN photocathode: Prospect for a high performance electron emitter," Ph.D. thesis, Stanford University, 2004.